Current Science
CS 5 (3), 3035-3044 (2025)
Received 26 **March** 2025 | **Revised** 25 **April** 2025 | **Accepted** 24 **May**. 2025 | **Online Available** 16 **June** 2025
https://doi.org/ 10.52845/CS/2025-5-3-73

Current Science

Current Science

OPEN ACCESS **ISSN(O)2795-8639**

Original Article

Multiscale Modeling and Hybrid Fuzzy Control of Decarburization in Grinding Hardening Processes

Xiao-Liang Shi[1,*] ·Xiao Liu[2]

[1]School of Physics, Liaoning University, Shenyang, 110819, China

[2]Library, Northeastern University, Shenyang, 110819, China

[*]Corresponding Author: Xiaoliang Shi, Xiao Liu

Abstract:
Decarburization significantly affects the surface properties of workpiece after grinding hardening. To effectively control the decarburization during grinding hardening, a comprehensive control model of carbon content on the surface of grinding-hardened workpiece is established based on molecular dynamics and a fuzzy logic algorithm. Based on the removal mechanism of grinding, a molecular dynamics model of grinding hardening is established, a mass of data of the decarburization of grinding hardening is obtained, and the data of surface roughness, hardness, and residual stress of workpiece are obtained through a grinding hardening experiment. Based on the model and experimental data, using the fuzzy logic control module of MATLAB, the forward and reverse fuzzy logic control models of decarburization are established. The forward model effectively estimated the integrity parameters of the machined surface. The reverse model can realize comprehensive control of decarburization, which ensures a reasonable range of decarburization under the condition that other machined surface integrity parameters are suitable for various working conditions
Keywords Grinding hardening, decarburization, molecular dynamics, surface integrity, fuzzy logic

1. Introduction

Grinding hardening is the combination of surface quenching and grinding[1]. By selecting an appropriate coolant dosage and grinding dosage and utilizing the large amount of heat generated during the grinding process, the surface temperature of the workpiece rapidly rises to the austenitizing temperature of the material and then cools rapidly, and the surface of the workpiece undergoes martensitic transformation, thus completing the quenching treatment of the workpiece surface[2]. Because the heat is mainly concentrated on the surface of the workpiece in the process of grinding hardness, the surface of the workpiece appears as a high-temperature field[3]; however, the influence on the interior of the workpiece is very small, and the thermal deformation of the workpiece after grinding hardness is very small[4]. At the same time, residual compressive stress appears on the surface of the workpiece owing to the phase transformation during the machining process, thereby improving the surface quality and service performance of the workpiece[5]. This technology can shorten the processing procedure of products, reduce production costs, and improve production efficiency, which is in line with the development strategy for energy saving and emission reduction[6]. Grinding hardening has opened up a research direction for integrated machining, which is convenient to introduce, has remarkable economic and social benefits, and has broad application prospects in the fields of metal material grinding and surface modification[7].

However, in the process of grinding hardening of carbon steel workpiece, owing to the large amount of grinding heat produced in the grinding contact area[8], the surface carbon elements easily react with oxygen and other components in the air under this high-temperature condition, resulting in the loss of carbon elements, that is, the decarburization phenomenon, and an obvious decarburization layer will be formed while the surface layer produces a strengthening effect. Surface decarburization behavior has an important influence on grinding and hardening[9]. After decarburization, the surface toughness of the workpiece is reduced, the surface became brittle, the fatigue strength is significantly reduced, and the service life of the workpiece is significantly shortened. The surface hardness decreased and the wear resistance is greatly weakened[10]. The original hardening effect is affected by grinding hardening[11].

Owing to the limitations of the machining mode and machine tool structure, it is very difficult to monitor the decarburization amount of the surface layer online[12]. When measuring the carbon content on the surface of workpiece after machining, the measurement also has high cost and multiple steps, and the measurement results of carbon elements are often discrete, random, and fuzzy because of the element characteristics and experimental principles[13]. Fuzzy control imitates the thinking mode of uncertain concept judgments and reasoning in the human brain[14]. For a description system with an unknown or uncertain model, fuzzy set and fuzzy rules are used for reasoning, and fuzzy comprehensive judgment is implemented, which is more suitable for controlling random and fuzzy decarburization behavior[15]. For this reason, this study establishes a decarburization self-adaptive fuzzy control model through the correlation fuzzy logic and grinding hardening decarburization model, changes the grinding parameters under the fuzzy rules, and realizes intelligent control of decarburization on the workpiece surface while ensuring machining quality.

2 Materials and Method

2.1 Molecular Dynamics Model of Grinding

In this study, LAMMPS molecular dynamics simulation software is employed to establish a grinding model for carbon steel material and simulate the degree of carbon loss, thereby obtaining the residual carbon content on the surface of the workpiece under different grinding parameters.

Initially, the initial conditions of the simulation system are set[16], including the designation of the simulation dimension as three-dimensional, with periodic boundary conditions in the X-direction and Y-direction and a free boundary in the Z-direction, and the selection of the metal unit system. The interactions between atoms are de-scribed using an atomic style, and parameters for generating the neighbor list and a time step of 0.001ps are set. The geometry of the workpiece region, including the boundary, thermostat, and Newton layers, is defined by combining the basic geometric shapes[17]. The material of the workpiece is set as 45 steel, which consists of iron and carbon atoms, with a body-centered cubic structure for its lattice. The grinding particle region is conical, composed of SiC atoms, and its lattice structure is specified through customization.

The atomic trajectory results are input into OVITO, and the visual result of the molecular dynamics simulation can be seen. The initial positions of the grinding particles and workpiece are shown in Fig. 1, with their relative positions defining the grinding depth.

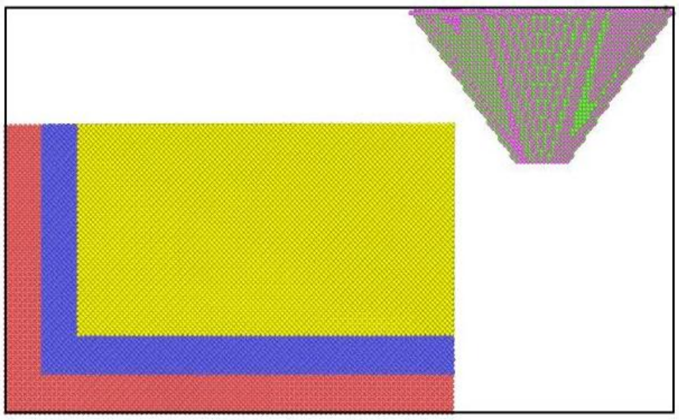

Figure 1 The initial positions of the grinding particle and workpiece

Before the simulation commenced, system initialization is performed, which included generating the simulation box and filling it with atoms, setting atomic masses, and grouping atoms for subsequent manipulation and analysis. The initialized model file is then saved. To simulate real physical processes, atoms in the boundary layer are fixed to prevent them from moving during the simulation. The FeC.eam potential function is used to describe the interactions between atoms. This potential function combines an embedding energy term and a pair potential term, enabling a good simulation of the physical and chemical properties of metallic materials. In the initial stage of the simulation, energy minimization is performed to ensure that the initial configuration of the system is in a stable energy state. Subsequently, the thermostat layer is initialized, set to an initial temperature of 20 °C, and relaxed to bring the system to a thermal equilibrium state. The workpiece region is further relaxed to eliminate potential internal stress.

In the grinding simulation stage, a certain velocity is imparted to the grinding particle, causing it to move along the negative X-axis direction. This velocity corresponds to the speeding speed of workpiece. Simultaneously, the thermostat layer is set to use the temperature-scaling method for temperature control to maintain a constant temperature during the simulation[18]. The workpiece region is set as a rigid body to simulate the fixed state of the workpiece during the actual grinding. The Newton layer is simulated using the NVE ensemble[19]. The compute command "compute car-bon-loss tool reduce sum C-count" is applied to calculate the number of carbon atoms in the grinding particle, and the variable "C-count" is used to store this value. The initial C content of the workpiece is 0.042%, according to the content of 45 steel. After simulation, the loss of carbon atoms is the output.

The simulation is run, and the simulation results are output, including the atomic trajectory file "cut.xyz" and the system status file "log.lammps."

2.2 Experiment of Grinding Hardening

45 steel is selected as the experimental material, which is the same as the model used in this study. The sample size is 60×15×15mm. A WE6800-ZC surface grinder is used for the grinding experiments. The grinding wheel is made of a white corundum ceramic. The grain size of the grinding wheel is F46, and its diameter is 250 mm. Reverse grinding is selected. The wheel speed is 40m/s. The grinding depth is from 100µm to 200µm. The feeding speed is from 0.01m/s to 0.03m/s. The grinding process is illustrated in Fig. 2.

Figure 2 Grinding hardening process

After the grinding hardening experiment, the workpiece is cut using wire electrode cutting to expose its section. The sections are then ground smoothly and slightly corroded in preparation for the subsequent detection. Elemental C is then tested using a JXA-8530F electronic probe. The roughness is measured using a TR3230 roughness tester. The surface roughness is measured by scanning the surface outline using a precise probe and the calculation. Hardness is measured using a THV-5 Vickers hardness tester. The load of the measurements is 1 kg. A LXRD-CHI X-ray diffraction tester is used to measure the residual stress of the workpiece after grinding. Before measurement, the surface of the workpiece is ground using abrasive paper and rinsed with absolute ethyl alcohol. Oxidation should be avoided during rinsing. The measurement location can be regarded as the surface layer of the workpiece.

3 Results and Discussion

3.1 Result of Molecular Dynamics Simulation

Fig. 3 shows the removal process of the material on the surface of the workpiece by the abrasive grains. A new surface is generated by the removal of the material.

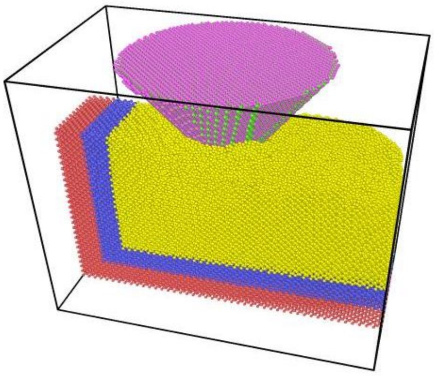

Figure 3 The visual result of the molecular dynamics simulation

The data of temperature of the simulation can be acquired from the system status file "log.lammps". Fig. 4 shows the temperature results of the surface layer when the grinding depth is 150μm. This reveals the variation in the thermal field with the movement of abrasive grains.

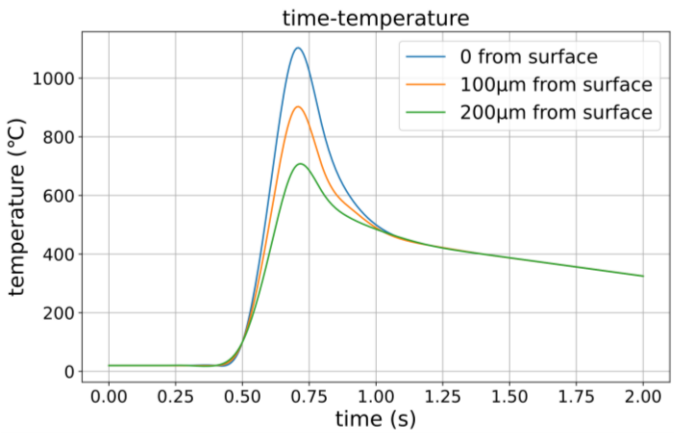

Figure 4 The temperature result of the surface layer when the grinding depth is 150μm

3.2 Results of C Content and Surface Integrity Parameters

The variable "C-count" after the simulation can be acquired from the system status file "log.lammps". Then the C content of the surface layer can be obtained from the simulation. The location which is 200μm from the surface under different grinding conditions shown in Tables 1. And the surface integrity parameters which is measured from experiment are also list here. It is the foundation of the fuzzy logic model.

By comparing the data for different grinding depths, it can be seen that the C content decreases with the increase in grinding depth. This is because greater grinding depths typically generate more grinding heat to achieve more obvious hardening effects. Under these conditions, the grinding temperature is higher. Therefore, at a larger grinding depth, decarburization is more obvious, and the C content is lower. By comparing the data for different feeding speeds, it can be seen that the C content increases with the increase in feed speed, but the increase range is small. This phenomenon is the result of the comprehensive action of grinding parameters. A higher feed speed usually produces more grinding heat and a higher grinding temperature, which enhances the C diffusion. However, a higher speeding speed also reduces the action time of the heat source, which is not conducive to the diffusion of C, and this effect plays a more important role. At very deep locations, the carbon content tended to remain constant. Other parameters have a similar trend due to the comprehensive effect of grinding force and heat.

Table 1 Result of C content, surface roughness, hardness and residual stress

a_p[μm]	v_s[m/s]	C content	roughness	hardness(HV)	residual stress(MPa)
100	0.01	0.32	1.226	243.7	11
	0.02	0.39	1.378	253.6	23
	0.03	0.41	1.389	270.5	20
125	0.01	0.28	1.306	252.6	90
	0.02	0.33	1.417	288.9	70
	0.03	0.39	1.459	288.3	98
150	0.01	0.07	1.355	296.7	101
	0.02	0.13	1.469	328.6	137
	0.03	0.17	1.486	339.2	135
175	0.01	0	1.386	340.1	116
	0.02	0	1.526	362.4	195
	0.03	0.02	1.537	379.5	180
200	0.01	0	1.581	365.6	242
	0.02	0	1.637	385.8	231
	0.03	0	1.852	397.1	257

Where, a_p represents grinding depth, v_s represents feeding speed.

4 Hybrid Fuzzy Control

4.1 Forward Fuzzy Control

MATLAB provides an excellent fuzzy control module. In this study, the fuzzy-logic module of MATLAB to establish a comprehensive decarburization control model[20]. The grinding depth and feeding speed are selected as inputs, the carbon content, surface roughness, hardness, and residual stress are selected as outputs, and a forward fuzzy control model is established. The Gaussian membership function is chosen as the membership function of the input fuzzy subset, which is not only widely used and has high stability but also has good resolution[21]. Because the feeding speed has little influence on decarburization, only three levels of feed speed are set in the training sample of the model, which are transformed into three areas: “large (L)”, “middle (M)” and “small (S)” through three membership functions. The grinding depth has a significant influence on the decarburization. For grinding depth, five membership functions are set, which correspond to five areas of “big”, “relative big”, “middle”, “relative small” and “small” after fuzzification.

According to the influence data of grinding parameters on decarburization and other machining quality parameters, combined with expert experience in the machining process, the following 15 control rules are established:

1) If (grinding depth is small) and (feeding speed is small), then (C content is high)(roughness is small)(hardness is small)(residual stress is small)

2) If (grinding_depth is small) and (feeding_speed is middle), then (C_content is high)(roughness is middle)(hardness is small)(residual_stress is small).

3) If (grinding_depth is small) and (feeding_speed is large), then (C_content is high)(roughness is moderate)(hardness is small)(residual_stress is small)

4) If (grinding_depth is relative_small) and (feeding_speed is small), then (C_content is middle)(roughness is middle)(hardness is small)(residual_stress is mid-dle).

5) If (grinding_depth is relative_small) and (feeding_speed is middle), then (C_content is high)(roughness is middle) (hardness is middle) (residual_stress is mid-dle).

6) If (grinding_depth is middle) and (feeding_speed is small), then (C_content is low)(roughness is middle) (hardness is middle)

(residual_stress is middle).

7) If (grinding_depth is middle) and (feeding_speed is middle) then (C_content is middle)(roughness is middle)(hardness is middle)(residual_stress is middle).

8) If (grinding_depth is middle) and (feeding_speed is large), then (C_content is middle)(roughness is middle)(hardness is middle)(residual_stress is middle).

9) If (grinding_depth is relative_large) and (feeding_speed is small), then (C_content is low)(roughness is medium)(hardness is medium)(residual_stress is me-dium).

10) If (grinding_depth is relative_large) and (feeding_speed is middle), then (C_content is low)(roughness is middle)(hardness is middle)(residual_stress is middle).

11) If (grinding_depth is relatively large) and (feeding_speed is large), then (C_content is low)(roughness is medium)(hardness is large)(residual_stress is medi-um).

12) If (grinding_depth is large) and (feeding_speed is small), then (C_content is low)(roughness is medium)(hardness is large)(residual_stress is large).

13) If (grinding_depth is large) and (feeding_speed is middle), then (C_content is low)(roughness is large)(hardness is large)(residual_stress is large).

14) If (grinding_depth is large) and (feeding_speed is large), then (C_content is low)(roughness is large)(hardness is large)(residual_stress is large).

15) If (grinding_depth is relative_small) and (feeding_speed is large), then (C_content is high)(roughness is moderate)(hardness is moderate)(residual_stress is moderate)

The set input is fuzzified by the membership function and solved. Finally, the specific value of the output is obtained by self-defuzzification using the fuzzy logic module in MATLAB. Fig. 5 shows a three-dimensional curved surface diagram of the influence law of each input quantity on the output quantity. It can be observed that the changing law agrees intuitively with the previous data of the model and experiment. Some areas in the figure are flat, reflecting the fuzzification of the fuzzy control model.

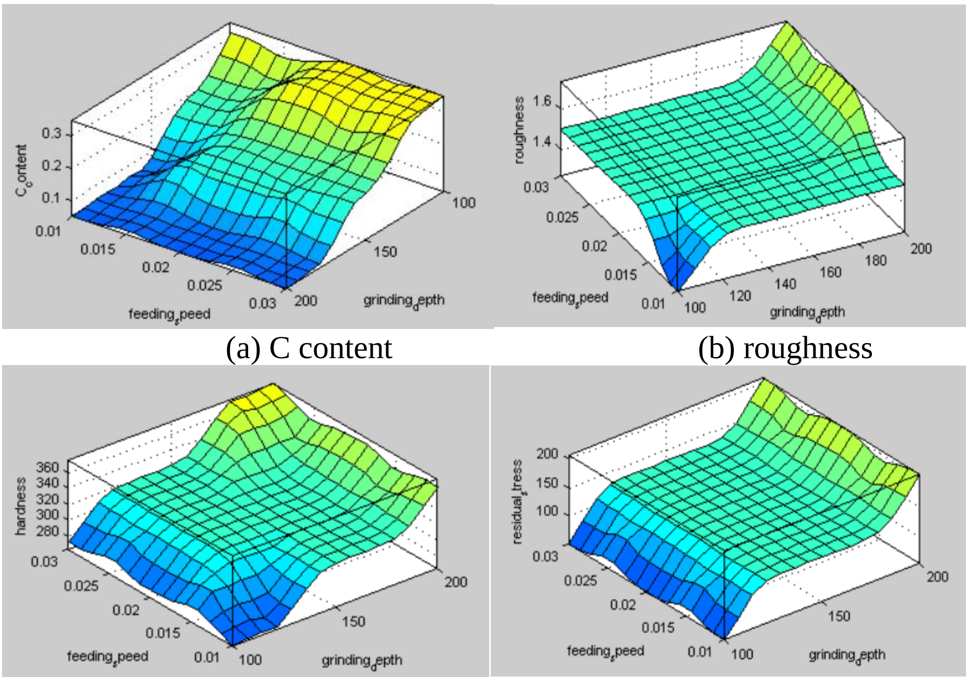

(a) C content (b) roughness

(c) hardness (d) residual stress

Figure 5. The relationship between surface integrity parameters and grinding conditions

Fig. 6 shows the screen of forward fuzzy logic control. Through setting the value of grinding depth and feeding speed, the value of C content, roughness, hardness and residual stress can be calculated through the fuzzy logic control model.

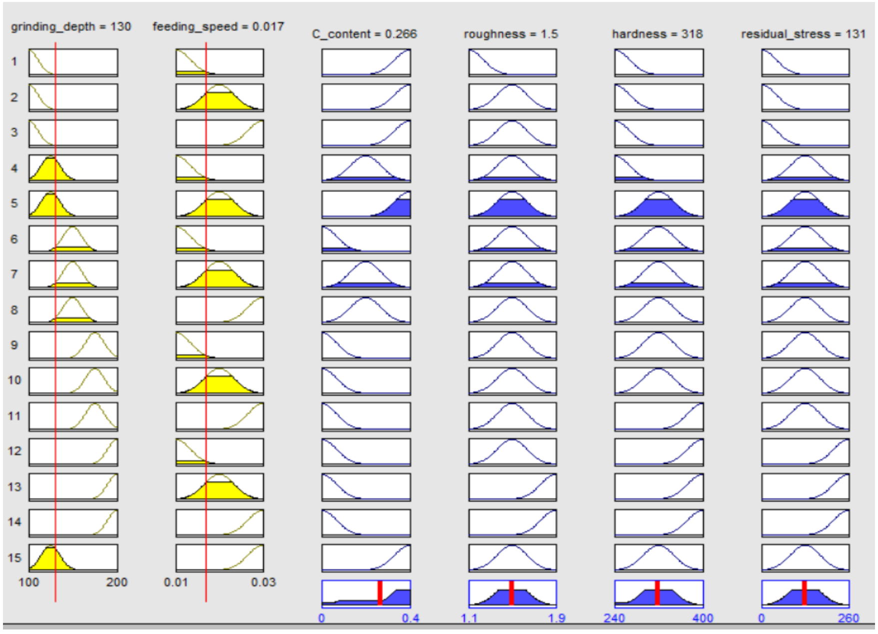

Figure 6. Forward result of fuzzy logic control

Table 2 presents a group of parameters which is obtained from the forward fuzzy logic control model as examples. It shows a comparison between the actual and estimated values of the fuzzy control model. The relative errors of estimation are less than 25%. In general, the error of the model is small. Here, the compared data of C content are from the calculation model because it is inconvenient to provide a mass of data, as mentioned above, and the measurement of C always has some error. Therefore, it does not make much sense to use experimental data for C content as for other measured items. The analysis takes the C data of the surface. If the decarburization of the inner layer needs to be analyzed, the method is the same after the C data of the surface are incorporated into the fuzzy control model.

Table 2 Comparison between the experiment value and the predicted value of the fuzzy control model(a_p=125mm, v_s=0.03m/s)

Item	Estimation of model	Compared data	error
C content	0.317	0.37	-14.3%
Roughness	1.492	1.459	2.3%
Hardness	319	288.3	10.6%
Residual stress	122	98	24.5%

4.2 Reverse Fuzzy Control

The carbon content, surface roughness, hardness, and residual stress are selected as inputs, and the grinding depth and feeding speed are selected as outputs. Then, a reverse fuzzy control model is established to set reasonable machining parameters under the condition of a proper level of decarburization and other machining quality characteristics. Three levels of carbon content, surface roughness, hardness, and residual stress are also set and transformed into three areas: “large (L)”, “middle (M)”, and “small (S)” by three membership functions. For grinding depth, five membership functions are set, which correspond to five areas of “big (B)”, “big”, “middle (M) ”, “small” and “small (S)” after fuzzification.

According to the related data of machining quality and grinding parameters, combined with expert experience of the machining process, fuzzy control rules are established[22]. In the case of three levels for each input quantity and four inputs, the control rules should be 3×3× 3×3, which is a total of 81 control rules. However, in the case of reverse control, some situations are inconsistent with the facts. For example, when the carbon content is high, the surface hardness cannot be very large because the grinding depth cannot be too large; that is, a large carbon content and large hardness do not coexist. There are several similar situations. After excluding all non-coexistence cases, the following 9 control rules remain, which are the control rules of reverse control:

1) If (C_content is small) and (roughness is middle) and (hardness is middle) and (residual_stress is middle), then (grinding_ depth is middle)(feeding_speed is small)
2) If (C_content is small) and (roughness is middle) and (hardness is middle) and (residual_stress is middle), then (grinding _depth is relative_large) (feeding_ speed is small)
3) If (C_content is small) and (roughness is middle) and (hardness is large) and (residual_stress is middle), then (grinding_ depth is relative_large) (feeding_ speed is middle)
4) If (C_content is small) and (roughness is middle) and (hardness is large) and (residual_ stress is middle) then (grinding_depth is relative_large) (feeding_speed is large).
5) If (C_content is small) and (roughness is medium) and (hardness is large) and (residual_stress is large), then (grinding_depth is large)(feeding_speed is small).
6) If (C_content is small) and (roughness is middle) and (hardness is large) and (residual_stress is large), then (grinding_depth is large)(feeding_speed is middle).
7) If (C_content is small) and (roughness is large) and (hardness is large) and (residual_stress is large), then (grinding_depth is large)(feeding_speed is large).
8) If (C_content is middle) and (roughness is small) and (hardness is small) and (residual_stress is middle), then (grinding_ depth is relative_small) (feeding_ speed is small)
9) If (C_content is large) and (roughness is small) and (hardness is small) and (residual_stress is small), then (grinding_depth is small)(feeding_speed is small).

Similarly, the set input is fuzzified by the membership function and solved, and finally, the specific value of the output is obtained by self-defuzzification using the fuzzy logic module of MATLAB. After the desired controlled quantity is input at the input end, the corresponding grinding parameters can be obtained at the output end, thereby obtaining the machining set value in advance. The core purpose of this study is to control decarburization. In the carbon content item, the required value is set according to the actual working conditions, and the corresponding parameters are set by considering the actual numerical requirements of surface roughness, hardness, and residual stress. The fuzzy solver can solve the required grinding depth and feeding speed under machining quality conditions. The following working condition is listed and analyzed as examples.

The workpiece must strictly control the decarburization. In addition, it requires very high machining precision and good wear properties. To obtain the mechanical properties after grinding hardening, the workpiece must maintain a large C content, small surface roughness, and high hardness. The C content is 0.35, roughness is 1.26, hardness is 351HV and residual stress is 101MPa. Subsequently, the required output is obtained. The grinding depth is approximately 126μm and the feeding speed is ap-proximately 0.022 m/s, as shown in Fig. 7.

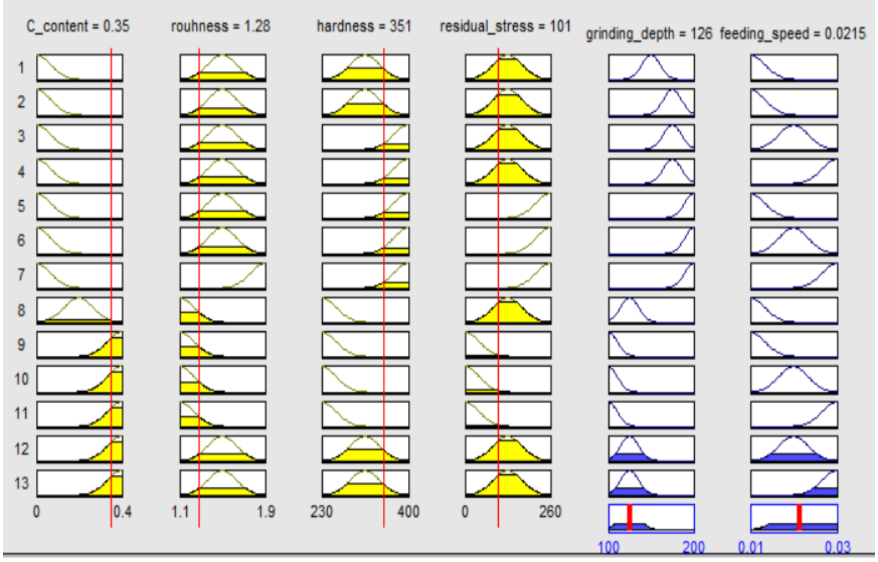

Figure 7 Control of decarburization with high machining precision and good wear property

5 Conclusion

Based on the removal mechanism of grinding, a molecular dynamics model of grinding hardening is established, and a mass of data on the decarburization of the surface layer of the workpiece of grinding hardening is obtained. The data and features of the surface roughness, hardness, and residual stress of the workpiece are obtained through a grinding hardening experiment.

The forward fuzzy logic model evaluates the surface characteristics, including the C content, roughness, hardness, and residual stress produced by the grinding hardening process, which has low estimated errors.

The reverse model can realize comprehensive control of decarburization, which ensures a reasonable range of decarburization under the condition that other machined surface integrity parameters are suitable for various working conditions.

Acknowledgements

This work was supported by the National Natural Science Foundation of China(52205452).

Reference

1. Jia, D.Z., Li, C.H., Zhang, Y.B., Yang, M., Zhang, X.P., Li, R.Z., Ji, H.J., Experimental evaluation of surface topographies of NMQL grinding ZrO2 ceramics combining multiangle ultrasonic vibration. *Int J Adv Manuf Technol*, 2019, 100(1-4): 457-473.
2. Mao, C., Liang, C., Zhang, Y.C., Zhang, M.J., Hu, Y.L., Bi, Z.M., Grinding characteristics of cBN-WC-10Co composites. *Ceram Int*, 2017, 43(18): 16539-16547.
3. Yamashita, A.S., Martins, W.T., Pinto, T.V.B., Raffo, G.V., Euzébio, T.A.M., Multiobjective Tuning Technique for MPC in Grinding Circuits. IEEE Access, 2023, 11: 43 041-43054.
4. Alonso, U., Ortega, N., Sanchez, J.A., Pombo, I., Izquierdo, B., Plaza, S., Hardness control of grind-hardening and finishing grinding by means of area-based specific energy. *Int J Mach Tools Manuf*, 2015, 88: 24 -33.
5. Mao, C., Ren, Y.H., Gan, H.Y., Zhang, M.J., Zhang, J., Tang, K., Microstructure and mechanical properties of CBN-WC-Co composites used for cutting tools. *Int J Adv Manuf Technol*, 2015, 76: 2043-2049.
6. Huang, X.M., Ren, Y.H., Zheng, B., Deng, Z.H., Zhou, Z.X., Experiment research on grind-hardening of AISI5140 steel based on thermal compensation. *J Mech Sci Technol*, 2016, 30(8): 3819-3827.
7. Zhang, Y., Ge, P.Q., Be, W.B., Plane grind-hardening distortion analysis and the effect to grind-hardening layer. *Int J Adv Manuf Technol*, 2015, 78(1-4): 431-438.
8. Shi, X.L., Liu, X., Research on Slight Decarburization Grinding Hardening based on the Gas-protecting Coupling Method. *CURR SCI INDIA*, 2024, 4(6): 894-902.
9. Thang, V.T., Tuan, N.A., Tiep, N.V., Evaluation of grinding wheel wear in wet profile grinding for the groove of the ball

bearing's inner ring by pneumatic probes. *J Mech Sci Technol*, 2018, 32(3): 1297-1305.
10. Nguyen, T., Zhang, L.C., Sun, D.L., Wu, Q., Characterizing the mechanical properties of the hardened layer induced by grinding-hardening. *Mach Sci Technol*, 2014, 18(3): 27 7-298.
11. Xiu, S.C., Shi, X.L., Transformation mechanism of microstructure and residual stress within hardening layer in pre-stressed dry grinding. *J Adv Mech Des Syst*, 2015, 9 (3): 15-00288.
12. Liu, B.S., Zhu, G.S., Li, H.X., Li, B.H., Cui, Y., Cui, A.M., Decarburization rate of RH refining for ultra low carbon steel. *Int J Miner Metall Mater*, 2010, 7(1): 22-27.
13. Liu, Y.B., Zhang, W., Tong, Q., Wang, L.F., Effects of Temperature and Oxygen Concentration on the Characteristics of Decarburization of 55SiCr Spring Steel. *ISIJ Int*, 2014, 53(8): 1920-1926.
14. Phu, N.D., Hung, N.N., Ahmadian, A., Senu, N., A New Fuzzy PID Control System Based on Fuzzy PID Controller and Fuzzy Control Process. *Int J Fuzzy Syst*, 2020, 22(7): 2163-2187.
15. Senthilkumar, P., Umapathy, M., Dhanalakshmi, K., Modulated adaptive fuzzy controller for position control of SMA wire actuator. *Int J Fuzzy Syst*, 2014, 27(1): 9-18.
16. Li, C., Hu, Y.X., Zhang, F.H., Geng, Y.Q., Meng, B.B., Molecular dynamics simulation of laser assisted grinding of GaN crystals. *Int J Mech Sci*, 2023, 239: 107856.
17. Chen, M.H., Dai, H.F., Molecular dynamics study on grinding mechanism of polycrystalline silicon carbide. *Diamond Relat Mater*, 2022, 130: 109541.
18. Ren, J., Hao, M.R., Lv, M., Wang, S.Y., Zhu, B.Y., Molecular dynamics research on ultra-high-speed grinding mechanism of monocrystalline nickel. *Appl Surf Sci*, 2018, 455: 629-634.
19. Shi, Z.M., Li, B.Z., Sun, Z.H., Study on microstructure evolution of grinding surface of bcc Fe-Ni maraging steel based on molecular dynamics. *Appl Surf Sci*, 2021, 57 3:151493.
20. Liu, Y., Adaptive-Fuzzy Control Compensation Design for Direct Adaptive Fuzzy Control. *IEEE Trans Fuzzy Syst*, 2018, 26(6): 3222-3231.
21. Capo-Lugo, P.A., Rakoczy, J., Fuzzy dipole magnetic control law. *Acta Astronaut*, 2019, 162:227-242.
22. Ku, C.C., Chang, W.J., Tsai, M.H., Lee, Y.C., Observer-based proportional derivative fuzzy control for singular Takagi-Sugeno fuzzy systems. *Inf Sci*, 2021, 570: 815-830.